3.4.2 CTSK2b1

A. Algorithm Outline

(1) Algorithm Code: CTSK2b1

(2) Product Code: SNGI, SNGI_p

(3) PI Name: Dr. Knut Stamnes

(4) Overview of Algorithm

The algorithm presented here for the retrieval of snow grain size, using GLI channels 5 (0.46 μm) and 19 (0.865 μm), is based on the principle that the reflectance of snow is known to be dependent on snow grain size in the near infra-red (NIR) range and pollution in the visible range. This algorithm works only under clear-sky conditions. It can be applied at high latitude (polar) as well as mid-latitude regions. In this algorithm several lookup tables have been constructed by using atmospheric optical properties obtained from MODTRAN in conjunction with the DISORT radiative transfer code. The bi-directional reflectance of snow is taken into account. In the lookup tables the radiances that would be measured by the satellite instrument are simulated as a function of snow grain size and mass fraction of soot mixed in the snow. The rationale behind the retrieval procedure of this algorithm is that the snow properties can be determined through a comparison of measured (by ADEOS-II/GLI) and simulated (the lookup table) radiance. The comparison will be done for GLI channels 5 and 19 in order to retrieve the mass fraction of soot and the snow grain size, respectively. The snow grain size and mass fraction of soot are obtained by requiring the simulated radiances to be consistent with the measured ones in both GLI channel 5 and channel 19. The retrieval of snow grain size is sensitive to the aerosol type. The effect of aerosol has been taken into account here. The tropospheric aerosol and Antarctic background aerosol models have been applied to the Arctic and Antarctic regions, respectively. The standard rural, urban, and Navy maritime aerosol models adopted from MODTRAN are employed for the mid-latitude area.

From Ver. 2 release new snow grain size retrieval algorithm at 1.64 μm is also considered to be included in the processing of global type product. We developed an algorithm, which is using GLI channel 28 (1.64 μm) independently to retrieve snow grain size at very top surface. Because the satellite measured reflectance at TOA (top of atmosphere) is no longer sensitive to snow impurity and aerosol properties at this wavelength, we can simply use the measured reflectance to retrieve snow grain size. It should be kept in mind, however, that this retrieved snow grain size is the grain at very top surface due to the very small penetration depth.

B. Theoretical Description

(1) Methodology and Logic Flow

1. Retrieval procedures

To relate the reflectance of snow to its physical properties such as grain size, the radiative transfer model has been used to generate a lookup table. In this lookup table, simulated radiances in GLI channels 5 and 19 have been calculated as a function of the snow grain size between 50 and 2000 μm and the mass fraction of soot ranging from 0.02 to 2.5 ppmw (parts per million by weight). Because the average grain size lies in the range 40-100 μm for new snow, 100-300 μm for fine-grained older snow, and 1000-1500 μm for old snow near the melting point, this table covers the range of snow grain sizes encountered in nature. Dependencies of the radiances on solar zenith angle (30-75°), sensor view angle (0-45°, according to GLI view angle), and relative azimuth angle between the sun and the sensor (0-180°) are also taken into account in the table. For each aerosol model, we have two look-up tables for retrieving grain size and soot, respectively.

We use lookup tables to maintain the accuracy of the retrieval and to save computation time. The retrieval is implemented by finding the best match between the measured satellite radiance for the pixel being analyzed in the GLI image and an entry in the lookup table. Lookup tables are generated by radiative transfer calculations for GLI channels 5 and 19, respectively. Figure 2.1 illustrates the reflected radiance in channels 5 and 19 as a function of the mass fraction of soot and snow grain size, and shows that the reflected radiance in channel 19 is generally more sensitive to snow grain size than to the amount of soot mixed in the snow. Therefore, the algorithm for retrieving snow grain size and soot mixed in the snow consists of three steps: (i) adjust the snow grain size in channel 19 until the computed TOA radiance agrees with the measured one; (ii) estimate the mass fraction of soot in the snow using the radiance of channel 5, after the grain size is determined from measurements 19; and (iii) compare the computed TOA radiances with the measured ones in channels 5 and 19, and, if inconsistent, repeat steps (i) and (ii) until the computed radiances agree with the measured ones for both channels 5 and 19.

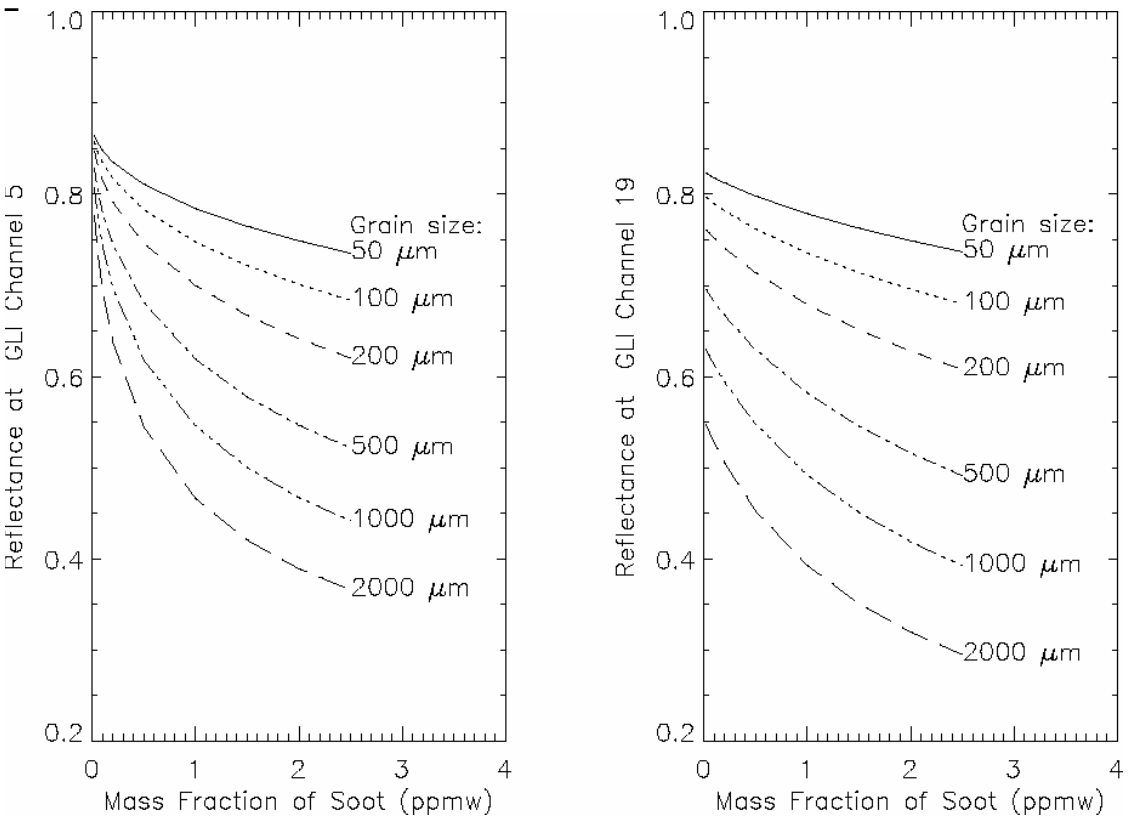

Figure 2.1
The reflected radiances of channels 5 and 19 as a function of the mass fraction of soot and snow grain size.

Figure 2.2 is a flow chart of the retrieval algorithm for snow grain size. The retrieval procedure of the algorithm can be summarized as follows:

1. Input the initial values of the snow grain size into lookup table 19, to provide a first estimate of the radiance in GLI channel 19.
2. Determine the snow grain size by adjusting it until the computed radiance from the lookup table agrees with the measured one in channel 19.
3. After the grain size is determined, the initial mass fraction of soot and the retrieved grain size are used as input to lookup table 5. Then the mass fraction of soot in the snow is determined by adjusting it until the computed radiance from the lookup table agrees with the measured one in GLI channel 5.
4. Use current grain size and soot as input to lookup table 19 and lookup table 5 to get the estimated radiances, and compare to the measured values at both channel 5 and channel 19. If inconsistent, go back to steps (1) and (2), and adjust grain size or soot until the estimated radiances agree with the measured results for both channel 5 and channel 19.

Thus, the final retrieval results will be obtained when the estimated radiances in both GLI channel 5 and 19 are consistent with the measured radiances. This retrieval procedure will be implemented for all snow-covered pixels under clear-sky conditions. A color picture with the distribution of snow grain size and soot will be generated by running the algorithm code to provide a visual display of the retrieval results.

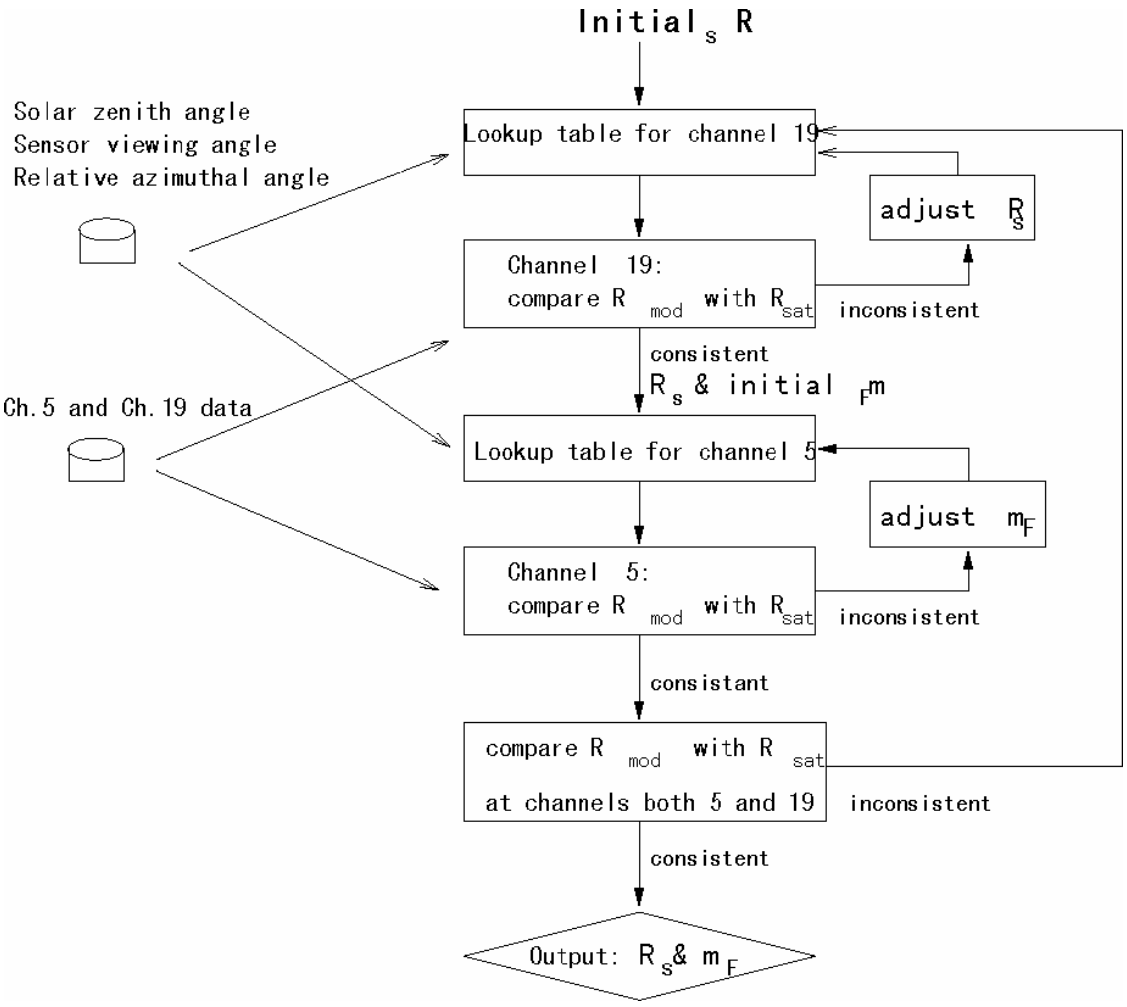

Figure 2.2
Flow chart of the retrieval algorithm for snow grain size and the mass fraction of soot. R_s is snow grain size, m_F is mass fraction of soot mixed in the snow, R_{mod} and R_{sat} are the radiances calculated from the model and measured by the GLI sensor, respectively.

Regarding the new algorithm which uses the GLI channel 28 (1.64 μm) for grain size retrieval, one corresponding lookup table "snow28.table" has been generated by using DISORT radiative transfer model pertinent of the coupled atmosphere-surface system.

In this lookup table, simulated reflectances in GLI channel 28 have been calculated as a function of the snow grain size between 50 and 2000 μm. There are 6 candidate snow grain sizes (50, 100, 200, 500, 1000, and 2000 μm). Dependencies of the radiances on solar zenith

angle (20-80 degree), sensor viewing angle (0-56 degree, for the GLI sensor), and relative azimuth angle between the sun and the sensor (0-180 degrees) are also taken into account in the table.

(2) Physical and Mathematical Aspects of the Algorithm

1. Background for snow grain size retrieval

It is well recognized that snow cover has a strong impact on the surface energy balance in any part of the world. Satellite remote sensing provides a very useful tool for estimating spatial and temporal changes in snow cover, and for retrieving snow optical characteristics. So far, Landsat TM (Thematic Mapper) data (Fily et al., 1997; Bourdelles and Fily, 1993) and AVIRIS (the Airborne Visible/Infrared Imaging Spectrometer) data (Nolin and Dozier, 1993; Painter et al., 1998) have been used for this purpose. Such retrieval is possible because snow reflectance depends primarily on the concentration of pollution (soot-contamination) in the visible range, but on snow grain size (Warren, 1982) in the near-infrared, as shown in Figure 2.3 (after Wiscombe and Warren, 1980).

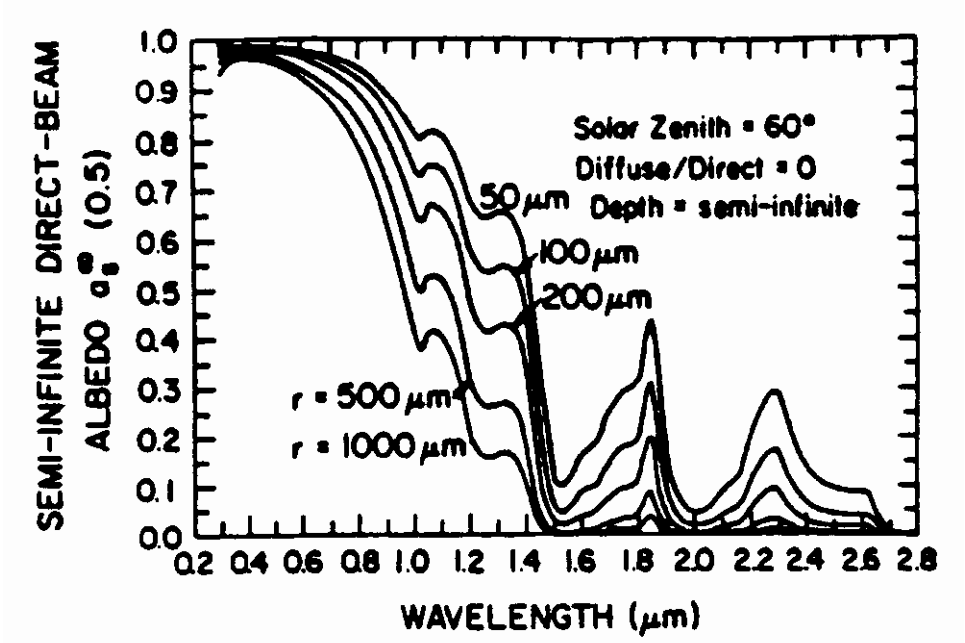

Figure 2.3 Spectra albedo of snow as a function of wavelength for grain size 50-1000 μm (after Warren and Wiscombe, 1980).

Nolin and Dozier (1993) estimated snow grain size using reflectance at 1.04 μm. However Bourdelles and Fily (1993) found that the grain size retrieved from Thematic Mapper band 4 (TM4) at 0.84 μm lies in the 420–430 μm range, which is much larger than the 145–165 μm grain size obtained from TM5 (1.65 μm) and TM7 (2.22 μm). They noted that retrieved size

depends on the radiation-penetration depth, which is wavelength-dependent. Fily et al. (1997) compared the in situ and Landsat TM-retrieved snow grain sizes and found that the in situ optical grain size is very different from the measured one at channels TM5 and TM7, but is close to the measured one at channel TM4. A linear relation between the measured grain size and optical size that depends on the wavelength has been used in their snow reflectance model.

While these previous studies have clearly shown that remote sensing holds promise for mapping snow grain size, they have also pointed to the need for appropriate instrumentation and development of inversion approaches to obtain quantitative snow grain size estimates. Pure ice is highly transparent in visible region, so that an increase in snow grain size has little effect on reflectance. However, because ice is moderately absorptive in the near-infrared, reflectance is sensitive to grain size, especially in the wavelength region 0.8-1.3 μm (Warren and Wiscombe, 1980) (Figure 2.3). For satellite measurements, the spectral channel should be located in a wavelength region where the effect of atmospheric scattering and absorption is negligible, so that when the radiance values are atmospherically corrected to yield surface reflectance, errors in the characterization of the atmosphere, particularly atmospheric water vapor, are minimized. For these reasons, GLI channels 19 (0.86 μm), 24 (1.05 μm), and 26 (1.24 μm) would be good choices for grain-size studies, because the grain-size effect is large when the effects of the atmosphere and snow impurities are small. The questions then arise: What is the difference among the retrieved grain sizes from different channels? How can we explain differences among the retrieved grain sizes? Which channel is the best choice for grain size retrieval? In an attempt to answer these questions, we have used AVIRIS data to study in more detail the physical meaning of the grain sizes retrieved from different channels. An important effect of the effective penetration depth of radiation has been revealed here (see section 3).

2. Snow reflectance model

As described above, snow reflectance is high in the visible part of spectrum and almost independent of grain size. In the NIR spectral region between 0.8 and 1.3 μm, snow has moderate reflectance that is very sensitive to the snow grain size (see Figure 2.3). This is why we expect GLI channels at wavelengths 0.86, 1.05, 1.24 μm to be useful for estimating the snow grain size. At wavelengths less than 0.8 μm, snow reflectance is affected by the presence of absorptive impurities as well as by grain size (Warren and Wiscombe, 1980). Therefore, visible radiation can be used to retrieve the snow impurities, while snow grain size can be determined using a channel in the range 0.8-2.5 μm. Figure 2.4 illustrates the reflectances at GLI channels 5 (0.46 μm) and 26 (1.24 μm) as a function of grain size and the soot mixed in the snow, respectively. Carbon soot contaminated snow was considered here.

Field measurements and model simulations indicate that snow exhibits significant bi-directional reflectance properties, which are more pronounced at large viewing angles. To relate the reflectance of snow to physical properties such as grain size, a comprehensive radiative transfer model based on the DISORT multiple scattering algorithm (Stamnes et al., 1988) has been applied to compute the bi-directional reflectance of the snow surface instead of assuming a Lambertian reflector. We employ the optical properties of pure snow obtained by Wiscombe and Warren (1980). Mie theory is used to get the extinction coefficient and the phase function, which means the snow grains are assumed to be spherical. The snow cover is considered as a homogeneous layer with a single grain size when we carry out the radiative transfer calculations. Of course, the real snow particles are not spherical. Thus, the particle

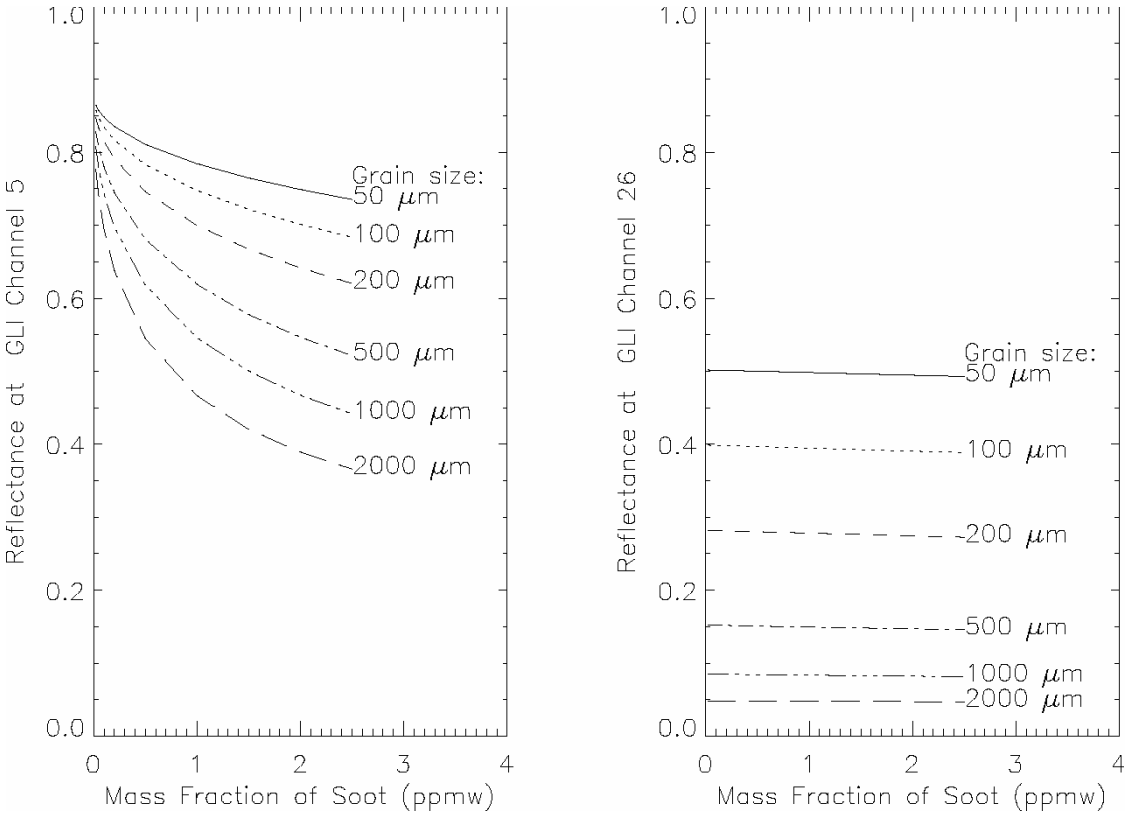

Figure 2.4
The reflectances of GLI channels 5 (0.46 μm) and 26 (1.24 μm) as a function of the mass fraction of soot and snow grain size.

radius used here is called the effective grain-size. It will generally be different from the measured grain size. Also these effective grain sizes represent depth-weighted-averaged values. The observing depth is dependent on the radiation penetration, which varies with wavelength.

In order to simulate atmospheric effect on the measured reflectance, the standard sub-arctic winter/summer and mid-latitude winter atmospheric profiles have been employed for polar and mid-latitude regions, respectively. For gases and aerosol, we adopt absorption and scattering properties for the GLI channels from MODTRAN. The tropospheric aerosol model and Aoki's

Antarctic background aerosol model (Aoki et al., 1999) have been used for Arctic and Antarctic regions, respectively. For the mid-latitude area, there are five different aerosol models employed: (i) rural aerosol model with 23 km visibility, (ii) rural aerosol model with 5 km visibility, (iii) navy maritime aerosol model with 10 (m/s) wind speed, (iv) urban aerosol model with 23 km visibility, and (v) urban aerosol model with 5 km visibility. The aerosol type for a given image will be automatically determined based on the measured reflectance difference between GLI channels 1 (0.38 μm) and 5 (0.46 μm). (See section 4).

3. Wavelength dependence of retrieved snow mean grain size

In order to compare the mean retrieved snow grain sizes from different channels, an AVIRIS image obtained at 22:45GMT on June 4, 1995 over the Arctic ocean was studied here. Using the method described above, the snow grain sizes were retrieved, as shown in Figures 2.5 a, b, c, and d for AVIRIS channels 54 (0.86 μm), 73 (1.05 μm), 93 (1.24 μm) and 145 (1.73 μm), respectively. Spatial variation of the retrieved snow grain size was independent of the wavelengths, but the magnitudes of the grain sizes retrieved from different channels were quite different. Figure 2.6 shows the retrieved grain size distribution for the whole image at each channel. The mean retrieved grain sizes were 1000, 550, 400, and 60 μm for channels 54, 73, 93 and 145, respectively. The longer the wavelength, the smaller the retrieved snow grain size. The mean grain size retrieved from channel 145 (1.73 μm) was too small to be reasonable. These differences could be due to the variable penetration depth of radiation depending on its wavelength as well as the grain size. What are the penetration depths of these channels? How can one explain the unreasonable grain size retrieved using channel 145? An explanation can be found by using the following two-layer snow model.

A two-layer snow model is adopted here to explore the effect of penetration depth of radiation on snow grain size retrieval. We assume that the thickness and snow grain size of the lower layer are 10 cm and 2000 μm, respectively. We then change the thickness and snow grain size of the upper layer to investigate the penetration depth and its variation with grain size at each channel. The penetration depth is defined as follows: when the upper layer becomes thick enough that the backscattered radiation is unaffected by the lower layer snow, and thus the snow albedo reaches a saturation value, we call this thickness the penetration depth. This is illustrated in Figure 2.7, which includes simulations for four different grain sizes (i.e. 100, 200, 500, and 1000 μm). Table 2.1 shows the penetration depth obtained from Figure 2.7 for different grain size at AVIRIS channels 54, 73, 93 and 145, respectively. We find that the penetration depth increases with increasing snow grain size, and decreases with increasing wavelength. As expected, the radiation penetrates deeper into coarse snow than into new snow.

Because the metamorphism induces the growth of the snow particles, the snow grain size generally increases with depth. Because of its greater penetration depth the measured reflectance from channel 54 is due to radiation backscattered by larger grains deeper within the snow than the radiation reflected at longer wavelengths. Thus, the grain size retrieved at channel 54 will be larger than those obtained from channels 73 and 93. The signals from channel 145 is only sensitive to the snow in a thin layer right below the surface. The grain shape may also have an important influence on the grain size retrieval. Aoki et al. (1998) found that at this wavelength (1.73 μm), the fine structure of the snow has a larger impact on

Table 2.1 The penetration depth as a function of snow grain size at AVIRIS channels 54, 73, 93 and 145, respectively

Snow grain size	Penetration depth (cm)			
(μm)	Ch. 54	Ch. 73	Ch. 93	Ch. 145
100	3.5	2.0	1.0	0.1
200	5.0	3.0	1.5	0.2
500	6.0	3.5	2.0	0.2
1000	6.5	3.5	2.0	0.2

snow reflectance than the crystal radius. For example, Aoki et al. found that at their observation site, the surface grain shape of the snow was dendrite. However, they found that the retrieved optical effective grain size corresponded to the branch size (25-50 μm) of the dendrite, rather than its crystal size (1000-2000 μm) . Thus, the effective grain size retrieved from channel 145 (1.73 μm) is quite different from those retrieved from channels 54, 73, or 93.

The differences among the retrieved snow grain sizes using AVIRIS channels 54, 73, and 93 are due to the different snow penetration depths at these wavelengths. The penetration depth is a function of wavelength and snow grain size. At AVIRIS channels 54, 73, and 93, the penetration depths are 3.5-6.5 cm, 2-3.5 cm, and 1-2 cm, respectively, depending on the snow grain size (see Table 2.1). The signal from channel 145 (1.72 μm) comes from a thin layer just below the snow surface. Therefore, we can conclude that: (i) the channel at shorter wavelength has a larger penetration depth than those at longer wavelengths; (ii) the penetration depth increases as the snow grain size increases; (iii) for the 1.73 μm wavelength

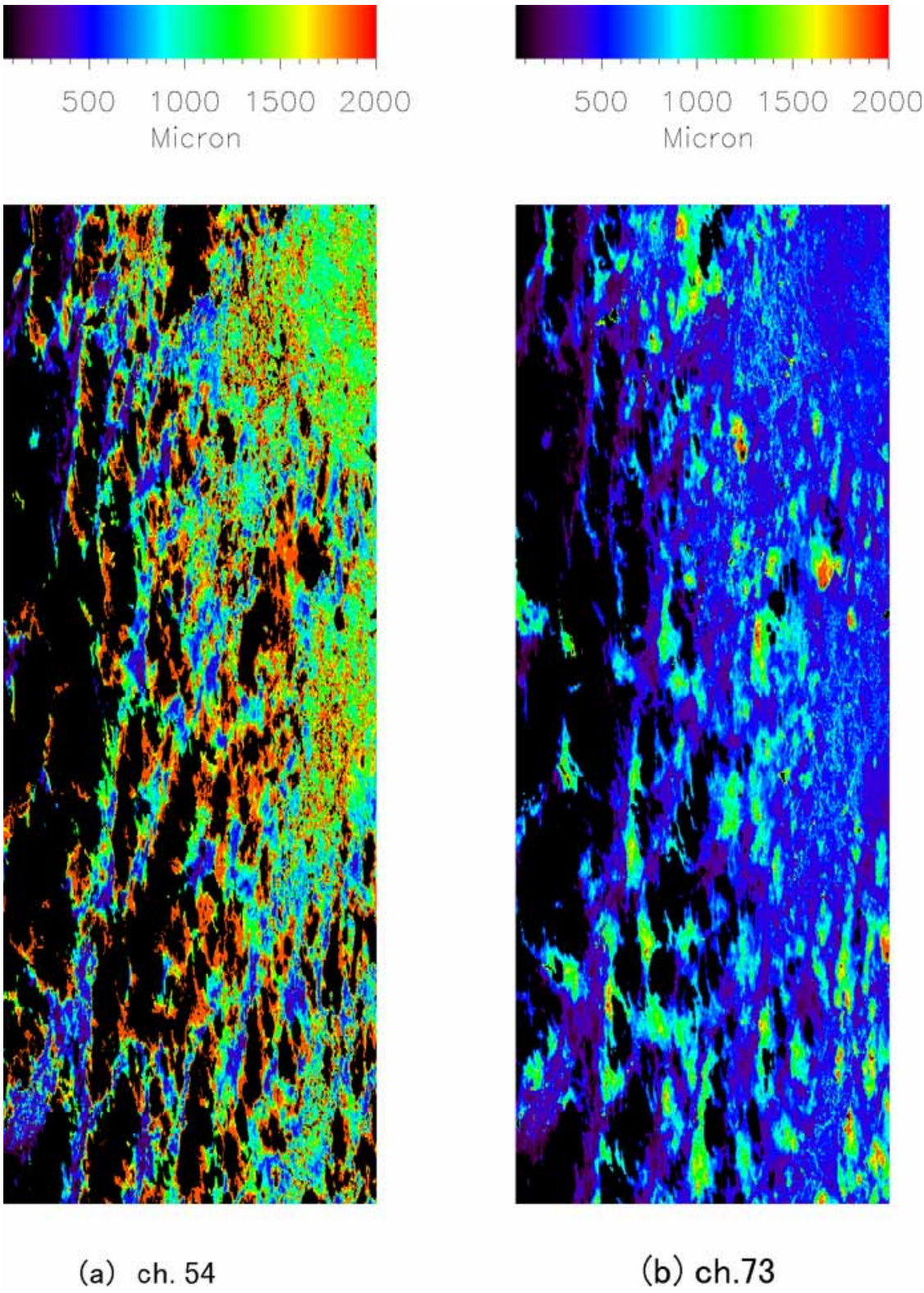

Figure 2.5 (a) & (b)
Retrieved snow grain size distribution at AVIRIS channels (a) 54 and (b) 73.

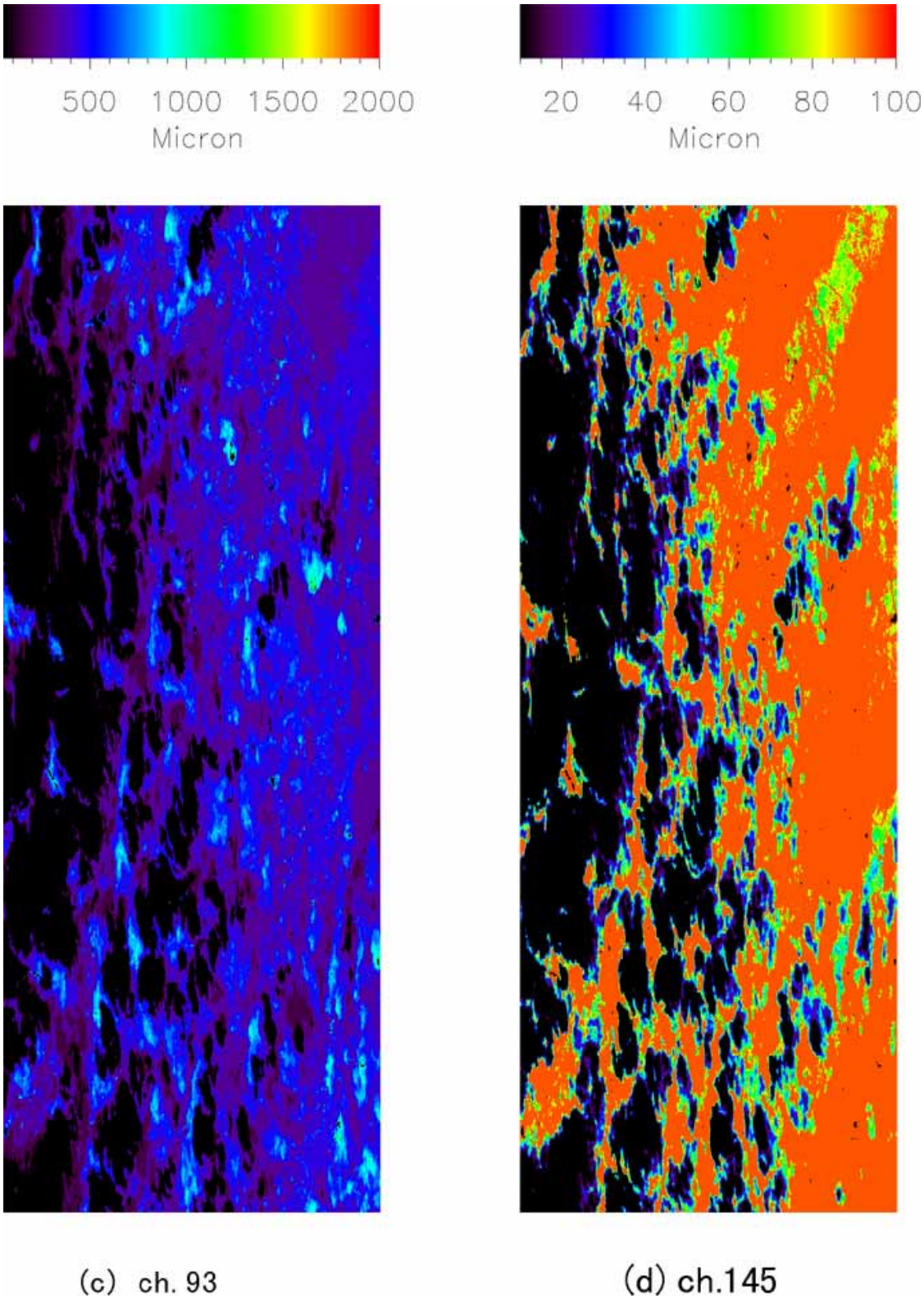

Figure 2.5 (c) & (d)
Retrieved snow grain size distribution at AVIRIS channels (c) 93 and (d) 145.

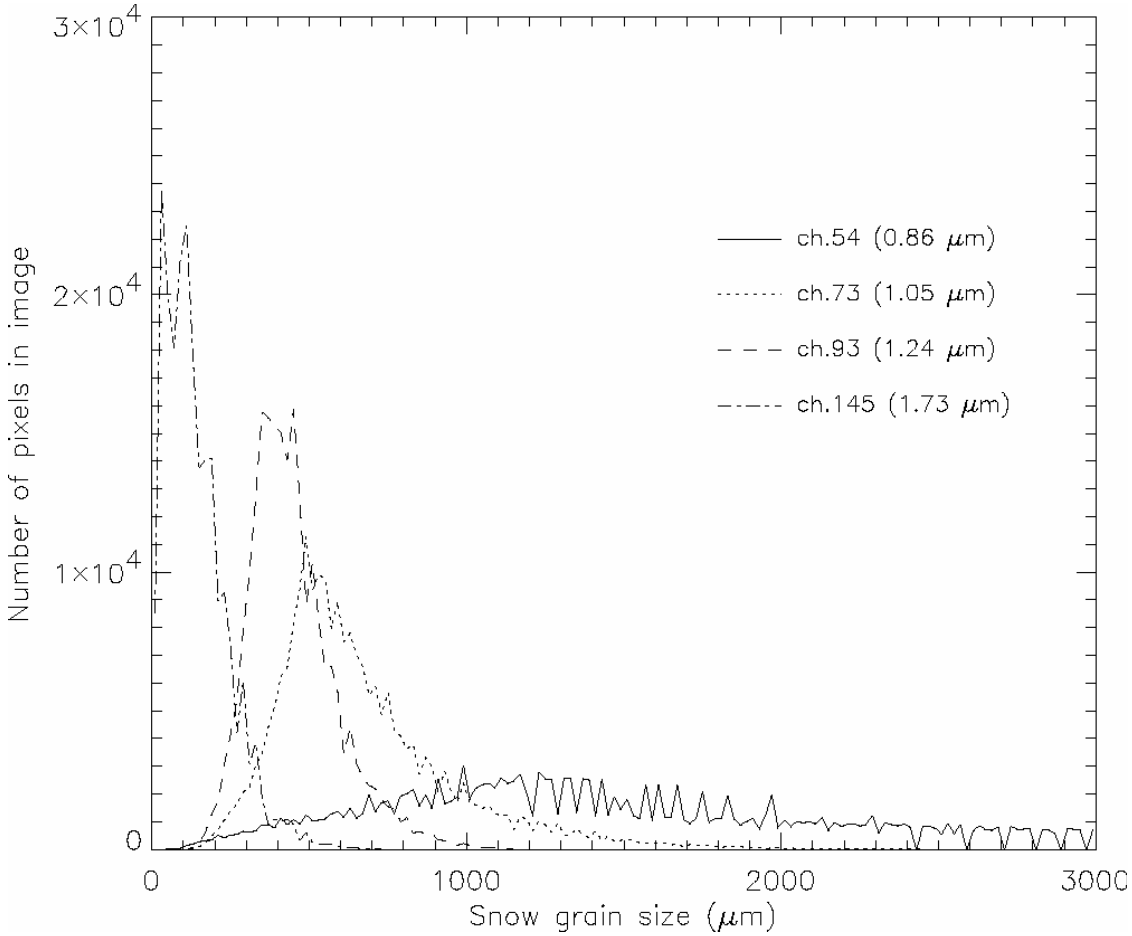

Figure 2.6 Histograms of retrieved snow grain size from AVIRIS channels 54, 73, 93, and 145.

channel, the signal comes from the snow surface and is very sensitive to the surface grain shape, making it difficult to estimate grain size at this channel, since the assumption of spherical particle shape may become invalid and the reflected radiation is more sensitive to fine structure (branch size) than to crystal size..

4. Channel selection for retrieving snow grain size and soot

Because the radiation penetration depths depend on wavelength, the mean retrieved snow grain sizes will depend on the channel selection. In order to retrieve consistent values of snow grain size and soot, we should choose wavelengths or channels with similar radiation penetration depth. For this reason, we select GLI channel 19 (0.865 μm) for snow grain size retrieval and channel 5 (0.46 μm) for soot retrieval. As already discussed, GLI channel 19 at wavelength 0.865 μm has penetration depths between 3.5 and 6.5 cm, depending on grain size, which is close to the penetration depth of GLI channel 5. MAS and AVIRIS data have been used for validation tests (see C. (2)). MAS channel 7 at 0.865 μm and AVIRIS channel 54 at 0.865μm are used for snow grain size retrieval, and MAS channel 1 at 0.546 μm and AVIRIS

channel 7 at 0.441 μm are used for retrieving soot mixed in snow. The characteristics of the corresponding channels of GLI, MAS, and AVIRIS are described in Table 2.2.

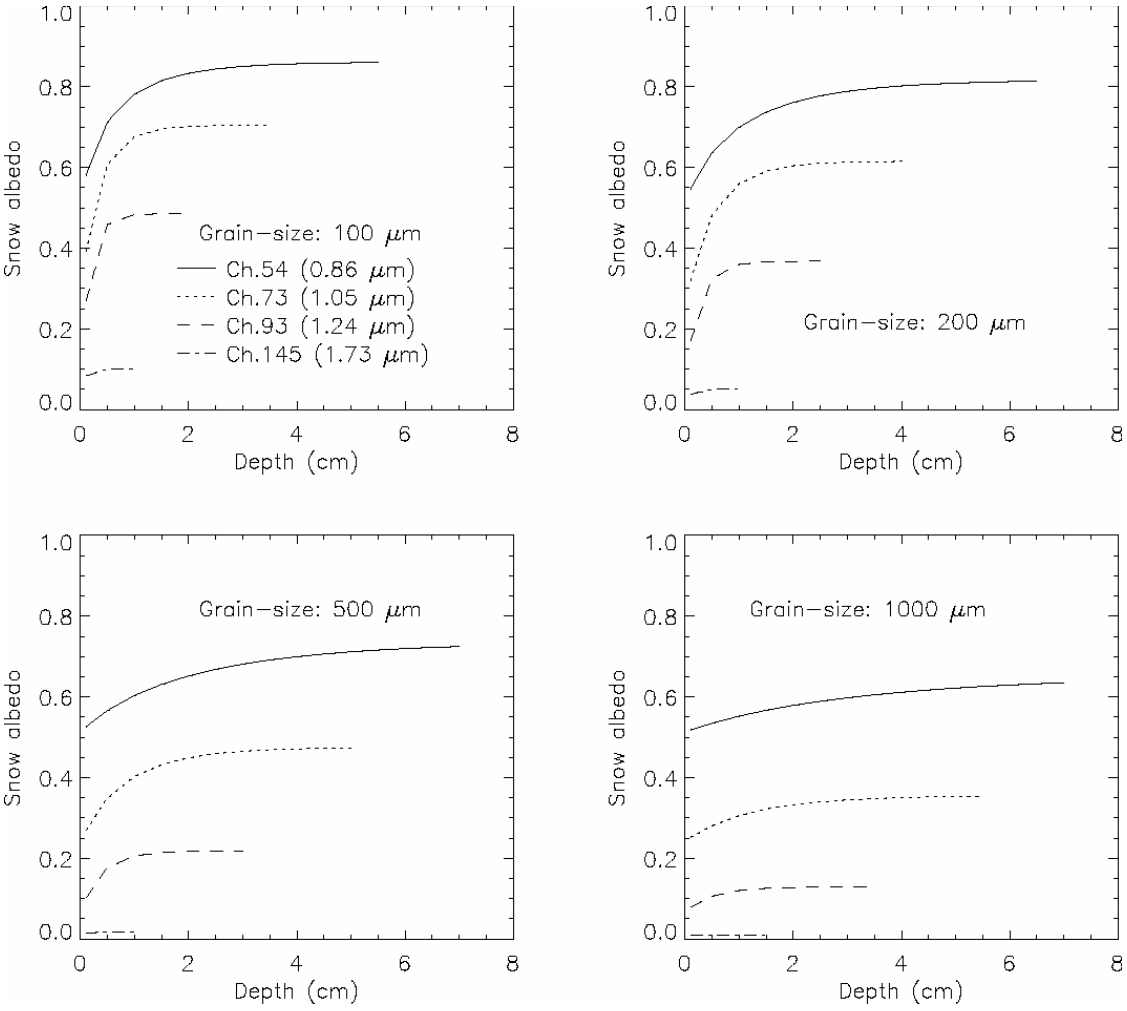

Figure 2.7 Computed snow albedo versus the depth of the upper snow layer for a two-layer snow model. The grain size and thickness of the lower layer are 2000 μm and 10 cm, respectively. The grain sizes inside the first layer are (a) 100 μm, (b) 200 μm, (c) 500 μm, and (d) 1000 μm, respectively.

Table 2.2 Comparison of channel characteristics

Sensor	Channel	Center position (μm)	Width (μm)
GLI	5	0.46	0.01
	19	0.865	0.01
MAS	1	0.546	0.046
	7	0.865	0.042
AVIRIS	7	0.44	0.01
	54	0.865	0.01

5. Selection of aerosol models

Aerosols play an important role in the snow grain size retrieval using ch.5 and ch.19 (not important for the grain size retrieval using ch.28). An unsuitable aerosol model adopted in the simulations would cause an error in the retrieved snow grain size. However, it is still a challenging issue to remotely sense and retrieve aerosol optical properties over snow surfaces. Aerosol model selection is one important part of the snow grain size retrieval algorithm discussed in this document.

For the Arctic area, we use the tropospheric background aerosol model included in MODTRAN in our algorithm, instead of Arctic haze, since the volume extinction coefficient of Arctic haze is similar to that of tropospheric aerosol (Blanchet and List, 1983). For the Antarctic area, we use an Antarctic background aerosol model (Aoki et al., 1999).

For mid-latitude areas we employ five aerosol models in our snow grain size retrieval algorithm. These aerosol models are: (i) rural aerosol model with 23 km visibility, (ii) rural aerosol model with 5 km visibility, (iii) Navy maritime aerosol model with 10 (m/s) wind speed, (iv) urban aerosol model with 23 km visibility, and (v) urban aerosol model with 5 km visibility. All data of these aerosol models have been provided using MODTRAN. Better choices of aerosol models can be included in future as deemed necessary based on the results of calibration and validation studies. If new aerosol models are included in the code there will be no changes in the algorithm except for some new lookup tables. To discriminate different aerosol models using satellite data, we employ the reflectance difference between GLI channels 1 (0.38 μm) and 5 (0.46 μm), based on the fact that the surface reflectance of snow stays almost constant in this spectral range. A reflectance difference between GLI channel 1 and channel 5 has been defined as follows:

$$R_1 - R_5 = a + bR_1$$

where the coefficients *a* and *b* depend on the aerosol model and geometrical data (such as solar zenith angle, view zenith angle, and relative azimuth angle). We have generated five lookup tables for aerosol model discrimination in mid-latitude areas. In these tables the coefficients *a* and *b* have been computed for five different aerosol models. The dependencies of the radiances on solar zenith angle, satellite viewing angle and relative azimuth angle between the sun and the satellite are also taken into account in the tables. For each clear pixel and sun-satellite geometry, the model reflectance difference between channel 1 and channel 5 (i.e. $R_1 - R_5$) is available from these lookup tables for each aerosol model (Figure 2.8). Comparing the measured $R_1 - R_5$ with the tabulated values allows us to determine which aerosol model provides the best match to the measurements for each pixel. Finally, one aerosol model for a particular image is determined from the pixel-by-pixel frequency of occurrence of these five aerosol models within the whole image.

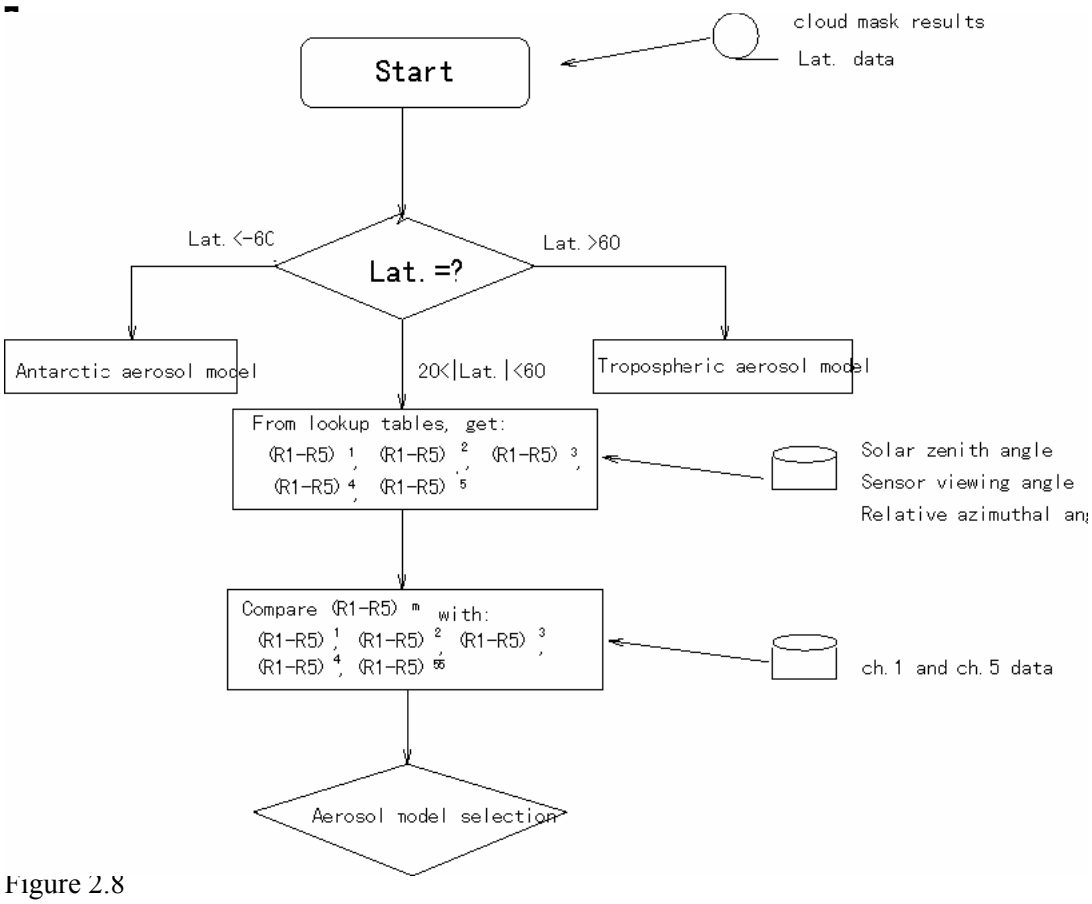

Figure 2.8
Flow chart for aerosol model determination. Here $(R_1 - R_5)^m$ is the measured-reflectance difference between channel 1 and channel 5, and $(R_1 - R_5)^1 - (R_1 - R_5)^5$ are the model-reflectance differences for aerosol models 1–5, respectively.

C. **Practical Considerations**

(1) Programming Requirements

The following table shows information about the expected software generated from this algorithm:

Table 3.1 Program Requirements

Program Memory	400 KBytes
Program Size	100 KBytes
Required Channels	1, 5, 19, 28
Necessary/Ancillary Data	
Expected Disk Volume	5 MBytes
Special Programs or Subroutines	gr_size.f, aermode.f
Look-up tables	5 look-up tables for aerosol model selection
	19 look-up tables for grain size and soot retrieval

(2) Calibration and Validation

In order to test the algorithm for the retrieval of snow grain size and mass fraction of soot in the snow, we applied it to MAS (MODIS Airborne Simulator) data and AVIRIS data. Two MAS data scenes were selected and processed. One is a scene observed over the Arctic Ocean,

the other is over Lake Erie. The AVIRIS data scene was obtained from the same NASA ER-2 flight as the MAS data over the Arctic Ocean. Although the ground resolution between AVIRIS and MAS is different, we can still compare the retrieved grain size and soot. AVIRIS provides us with more appropriate channels that are at the same wavelengths as the GLI channels. As we discussed in section B. (2) 3, AVIRIS data also provides a good opportunity to test the wavelength dependence of our snow grain size retrieval algorithm. Further, a simulated GLI image generated by the DISORT radiative transfer model has been used here to provide a necessary test of our algorithm.

The implementation of the algorithm will follow the flow chart in Figure 2.9. First, we apply the cloudy/clear discriminator and snow/sea-ice discriminator to the MAS imagery, to distinguish cloud from snow or other types of surfaces, in each pixel. Under clear-sky conditions, this algorithm can be used to retrieve the snow grain size for all snow-covered pixels. For MAS data, MAS channel 1 (0.546 μm) and 7 (0.865 μm) is employed, instead of the GLI channels 5 and 19, to retrieve the snow grain size and the amount of soot mixed in the snow. For AVIRIS data, AVIRIS channels 7 (0.441 μm) and 54 (0.865 μm) are used for this purpose.

The output of this algorithm to determine snow grain size and mass fraction of soot are two binary data stored in a HDF file. If a pixel is not classified as "snow" by the cloudy/clear and snow/sea-ice discriminators (cf. ATBD for CTSK1a and CTSK1b submitted to NASDA by Knut Stamnes, PI of the contract G-0052 for GLI program, 1999), the number 4000 is assigned to this pixel in the output file. We assume that the grain size of a snow pixel should normally lie between 10 and 3000 μm, with soot content between 0 and 3 ppmw. If a snow pixel has grain size or soot outside these ranges, the number -1000 is assigned for this pixel, implying that the measured value for this pixel is a *bad* data point. A brief description of the output data is given in Table 3.2. These output files "grain.data" and "soot.data" are used for the computation of surface albedo. The frequency distributions of snow grain size and soot for the given image are also output.

Table 3.2 Description of the data values for the output

Data value	Meaning
-1000	bad data for grain size in the snow-covered pixel
-1000	bad data for soot in the snow-covered pixel
10-3000	snow grain size retrieved from 865nm channel
	snow grain size retrieved from 1.64μm channel
0 - 3	mass fraction of soot in the snow-covered pixel
-4000	non-snow-covered pixel

1. Application to AVIRIS data

We use data obtained during the ARMCAS (Arctic Radiation Measurements in Column Atmosphere-Surface) field experiment on June 4, 1995 over the Arctic ocean near Prudhoe Bay (70°31'33", 147°08'23"). The instrument AVIRIS was flown on the NASA ER-2 flight at an altitude of 20 km. It is an airborne imaging spectrometer with 224 contiguous spectral channels from 0.4 μm to 2.45 μm, with a spectral response function of 10 nm. The field-of-view (FOV) is 10.5 km and the ground resolution is 20 m.

Generally, the relationship between snow reflectance at satellite level and snow grain size, depends on both the solar and viewing geometries. AVIRIS is a nadir viewing instrument. Its FOV is only 10.5 km. Thus, for AVIRIS data, only the solar zenith angle is required to calculate the bi-directional reflectance. Figure 3.1 shows curves of the simulated reflectance versus the equivalent snow grain size for AVIRIS channels 54, 73, 93 and 145, at the solar

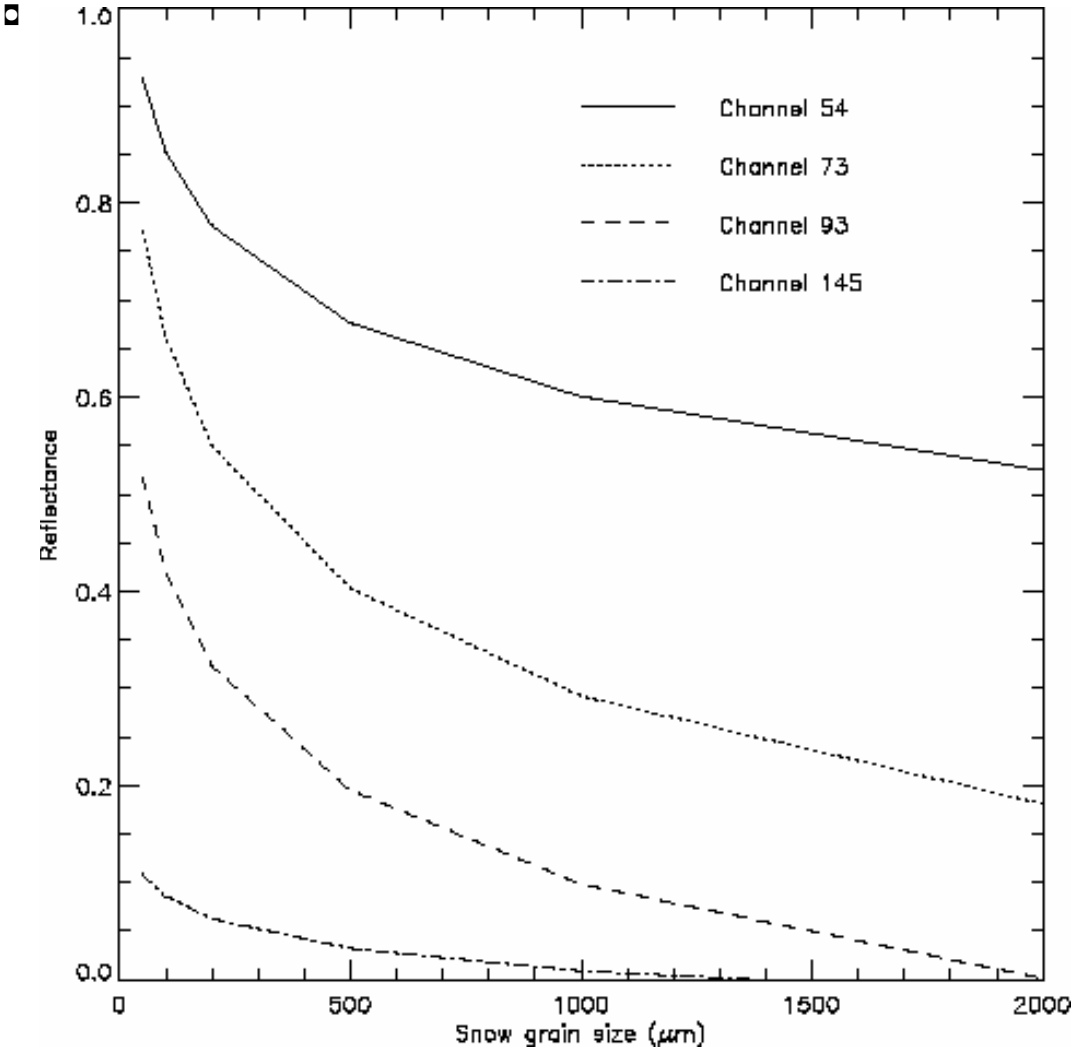

Figure 3.1 Simulated reflectance as a function of effective snow grain size for a solar zenith angle 49°.

zenith angle 49°, which is the solar zenith angle for the scene shown. We can simply use these curves, instead of the lookup tables, to estimate the grain size for the acquired image.

According to the method described above, the retrieved snow grain size and soot of the image are shown in Figure 2.4 for AVIRIS channels 54, 73, 93 and 145.

2. Application to MAS data

Here are two cases for the application of algorithm to MAS data in the Arctic and mid-latitude regions. First, we show one MAS observation made on June 4, 1995 (track 6) over the Arctic Ocean near Prudhoe Bay, Alaska. This scene was obtained simultaneously with the AVIRIS data shown above. So a comparison between MAS and AVIRIS retrievals is presented here. The snow grain size for the full image is plotted in Figure 3.2 to show the spatial distribution of the retreived grain size. Different colors are used to represent the different snow grain sizes, as indicated in Table 3.2. Please note that the black area indicates the non-snow-covered pixels or points with bad data.

In Fig. 3.2, the red square box indicates the area that the AVIRIS data covered in Fig. 3.1. Comparing the retrieved snow grain size from AVIRIS data in Fig. 3.1 with that from MAS data in Fig. 3.2, the retrieved snow grain size region from MAS data is consistent with the result from AVIRIS data. The mean retrieved grain sizes are around 1000 μm for using both data, although the ground resolution (50 m) and channel width (0.04 μm) of MAS are different from that of AVIRIS (20 m for ground resolution, 0.01 μm for channel width). Thus, the algorithm has been successfully applied to different data from different instruments with very good agreement.

Another case is MAS observation obtained over Lake Erie on February 9, 1997 (track 3). This is an example of applying the algorithm to mid-latitude areas. Navy maritime aerosol model has been used here. The mean retrieved grain size and soot are about 500 μm and 1.0 ppmw, respectively, as shown in Fig. 3.3.

3 Application to a simulated GLI image

A simulated GLI image has been generated, using the DISORT radiative transfer model. In this image, we have included snow, land, ice cloud and water cloud pixels, respectively (see Fig. 3.4). The upper part of image is under clear sky condition, and the lower part of image is under for cloudy sky condition. We have also assumed that this image was observed in summer in the Arctic region, with a solar zenith angle of 60°. So the summer Arctic aerosol mode is used to retrieve snow grain size and mass fraction of soot mixed in the snow.

First, the cloud/clear and snow/sea-ice discriminator is applied to this image to obtain the result of cloud mask. The left panel of Fig. 3.5 shows the true data when we generated the simulated GLI image (i.e. the input for forward simulation). The result of cloud mask with

applying the cloud/clear and snow/sea-ice discriminator is shown in the right panel of Fig. 3.5. The colors in Fig. 3.5 have been described in Table 3.3. From Fig. 3.5, we can find that the cloudy/clear and snow/sea-ice discriminator algorithm works well for most pixels, with the exception of some water cloud pixels.

The second step is to retrieve the snow grain size and mass fraction of soot mixed in the snow. Fig. 3.6 shows the true data of the grain size and soot when we generated the simulated GLI image in the left panel and right panel, respectively (i.e. the input for forward simulation). The results of retrieved snow grain size and mass fraction of soot mixed in the snow are shown in the left and right panels of Fig. 3.7, respectively. Comparing Figs. 3.6 and 3.7, we have obtained the relative retrieval error, as shown in Fig. 3.8. For snow grain size retrieval, there are about 81% pixels with the relative retrieval error less than 10%; and about 19% pixels with the relative retrieval error in the range 10-30%. The larger relative error has occurred in the pixels with small grain size (50 μm) and small soot (0.02 ppmw) or large soot (2.5 ppmw). For the retrieval of mass fraction of soot mixed in the snow, there are about 83% pixels with relative error less than 10%, and 17% pixels with the relative error in the range 10-18% . The larger relative error has occurred in the pixels with larger soot (2.5 ppmw) or smaller soot (0.02 ppmw). Generally speaking, in Arctic region the snow grain size lies in range from 100 to 1000 μm, and soot in the range from 0.1 to 0.5 ppmw. Thus, the relative retrieval error usually should be less than 10%.

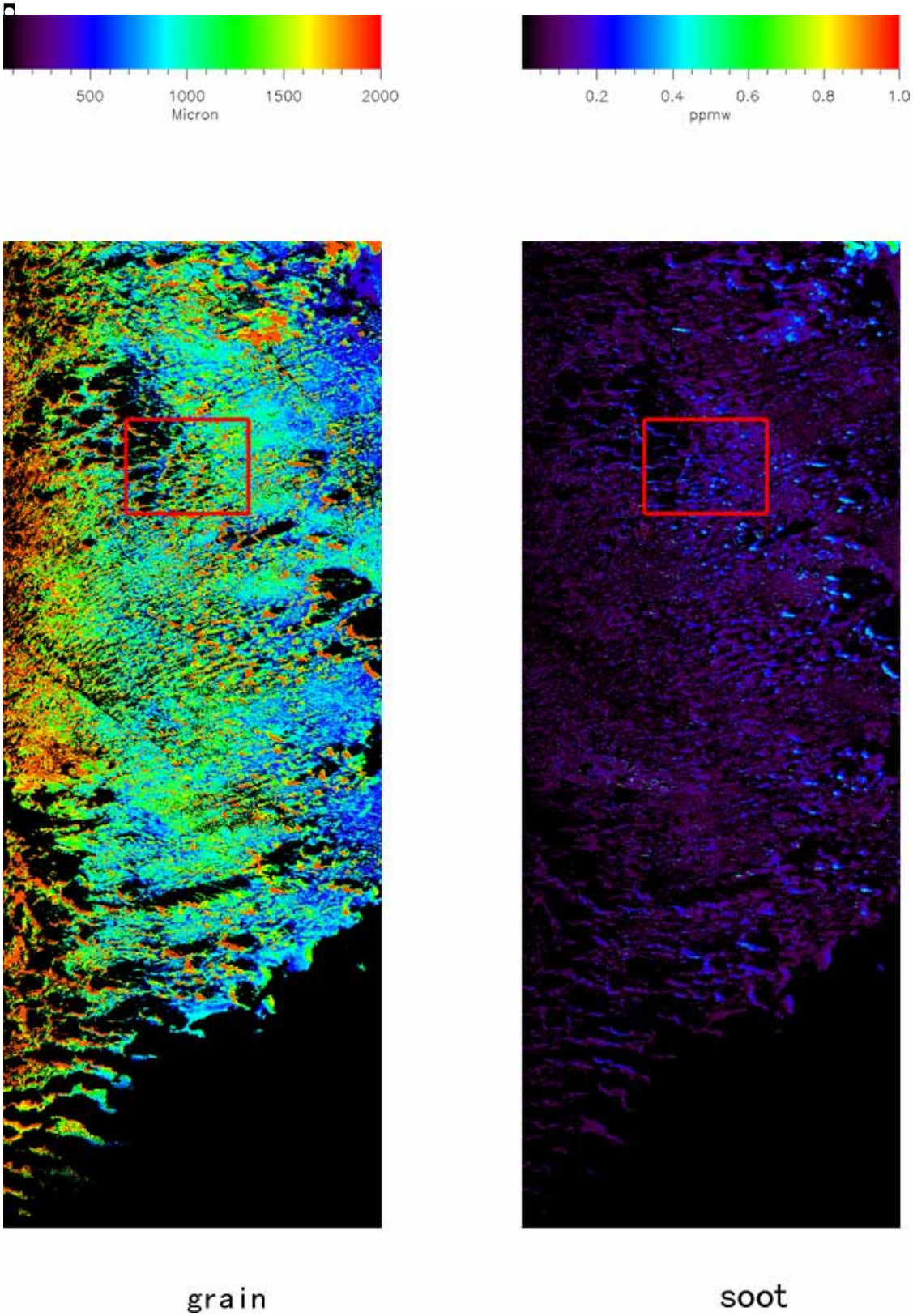

Figure 3.2
Retrieved snow grain size and soot distribution on June 4, 1995, over the Arctic Ocean.

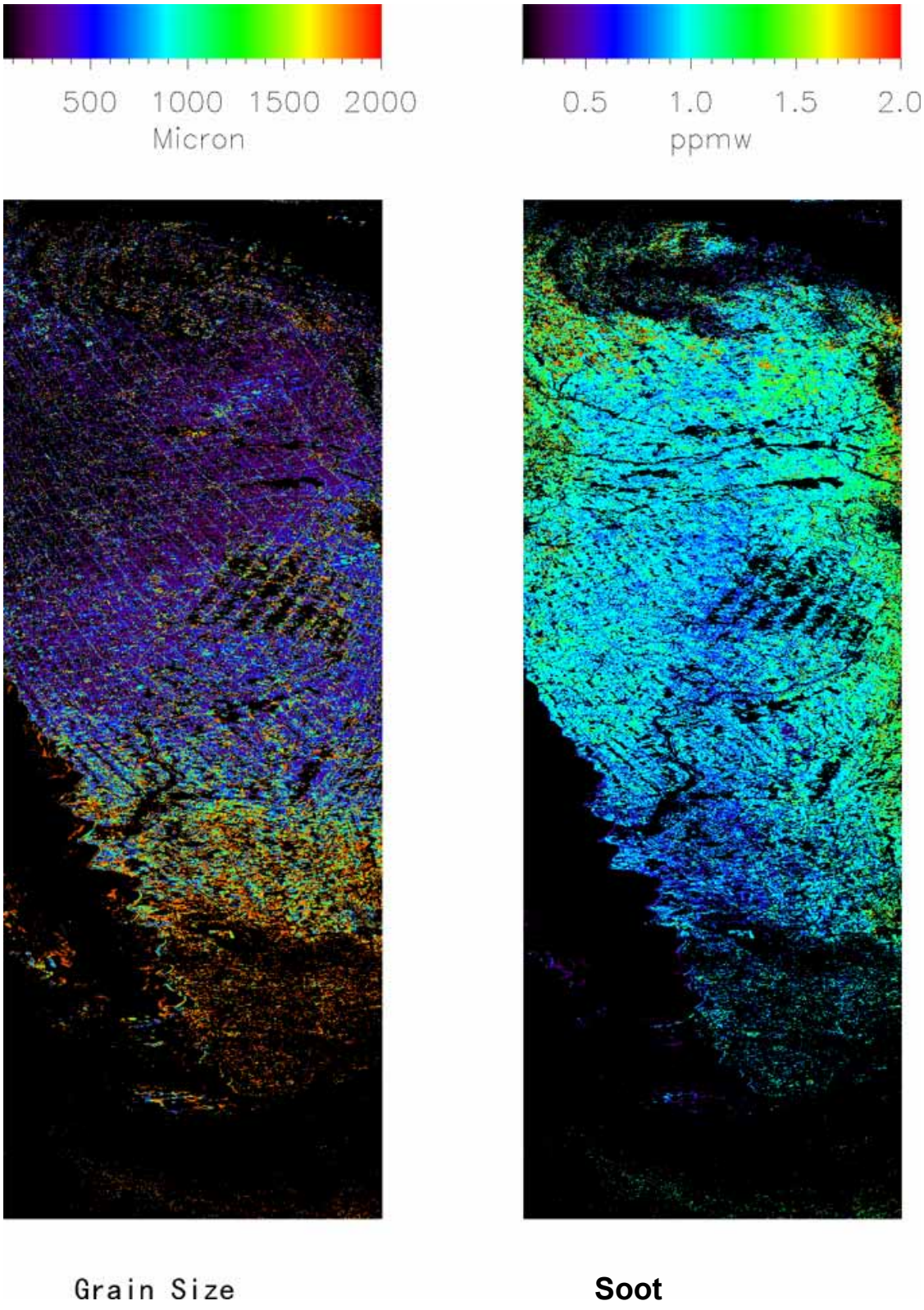

Figure 3.3
Retrieved snow grain size and soot distribution on Feb. 9, 1997, over Lake Erie.

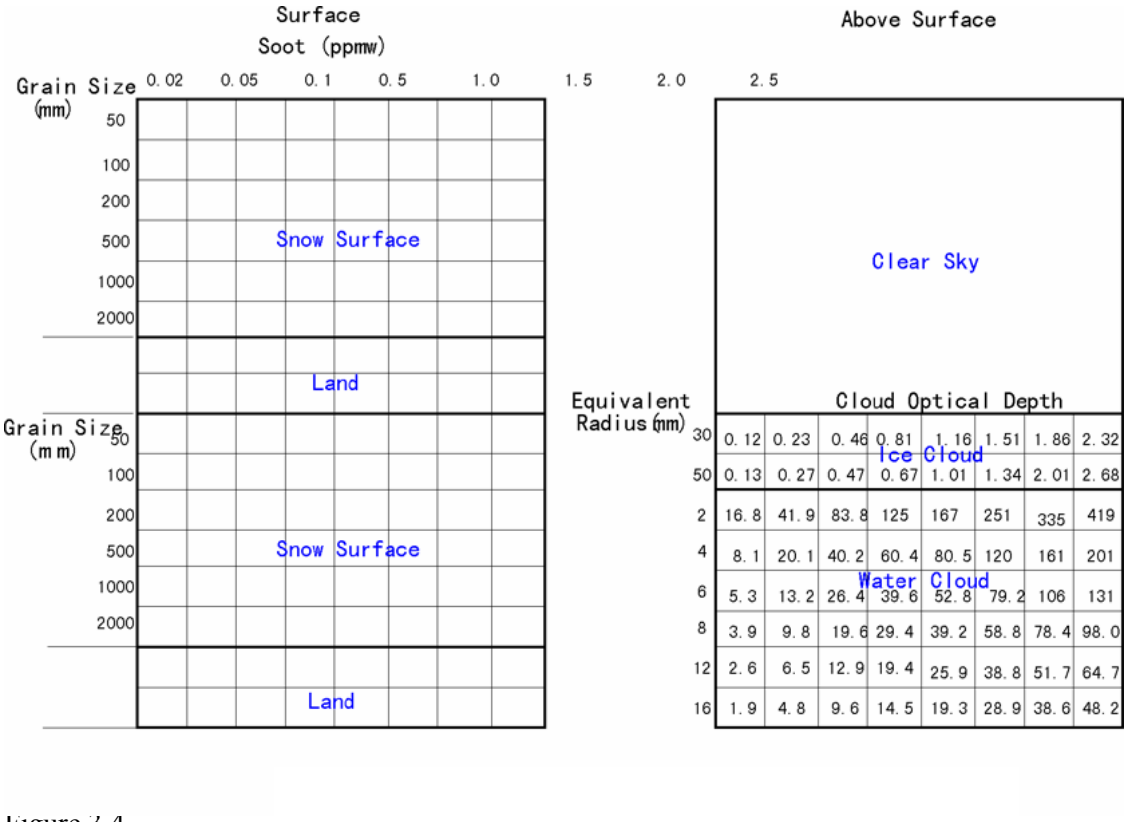

Figure 3.4
The structure of the simulated GLI image.

Table 3.3 Description of colors in cloud mask image

color	**meaning**
red	snow over ocean
blue	sea-ice
yellow	land
green	high confidence cloud
sea green	middle confidence cloud
coral	low confidence cloud
magenta	snow over land
cyan	water

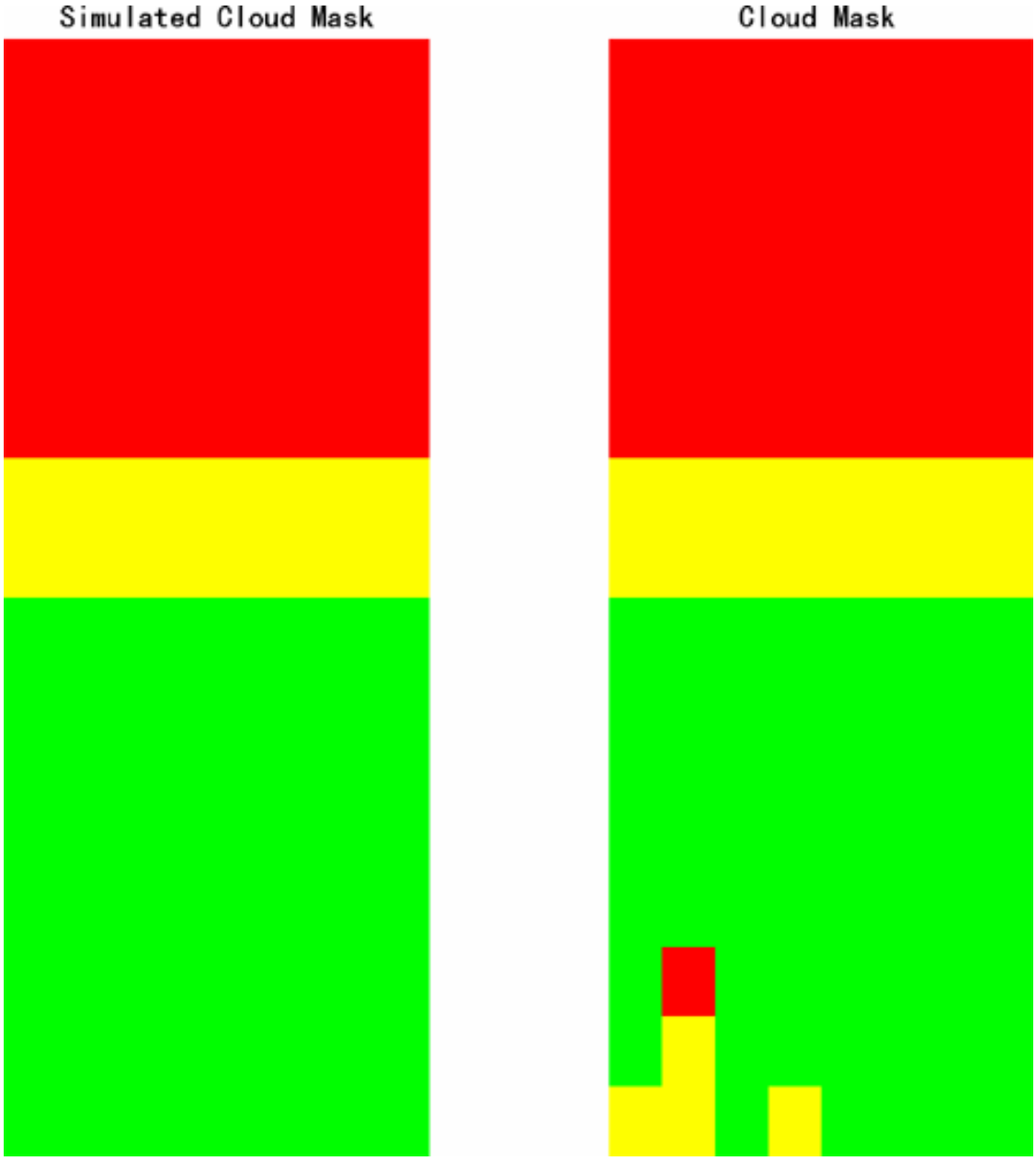

Figure 3.5
The cloud mask for true data (left panel) and result data (right panel).

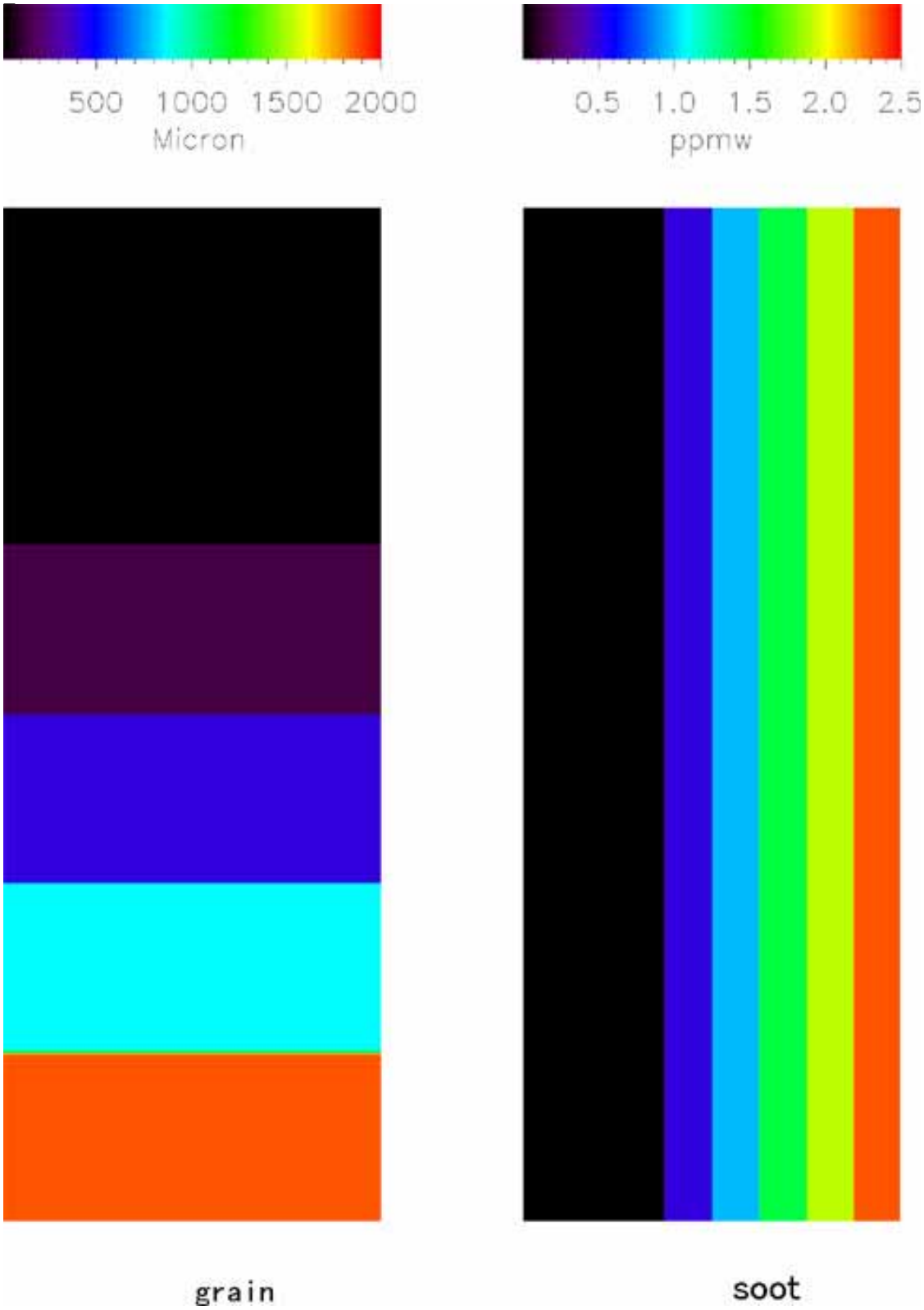

Figure 3.6
Snow grain size (left panel) and mass fraction soot mixed in snow (right panel) for true data.

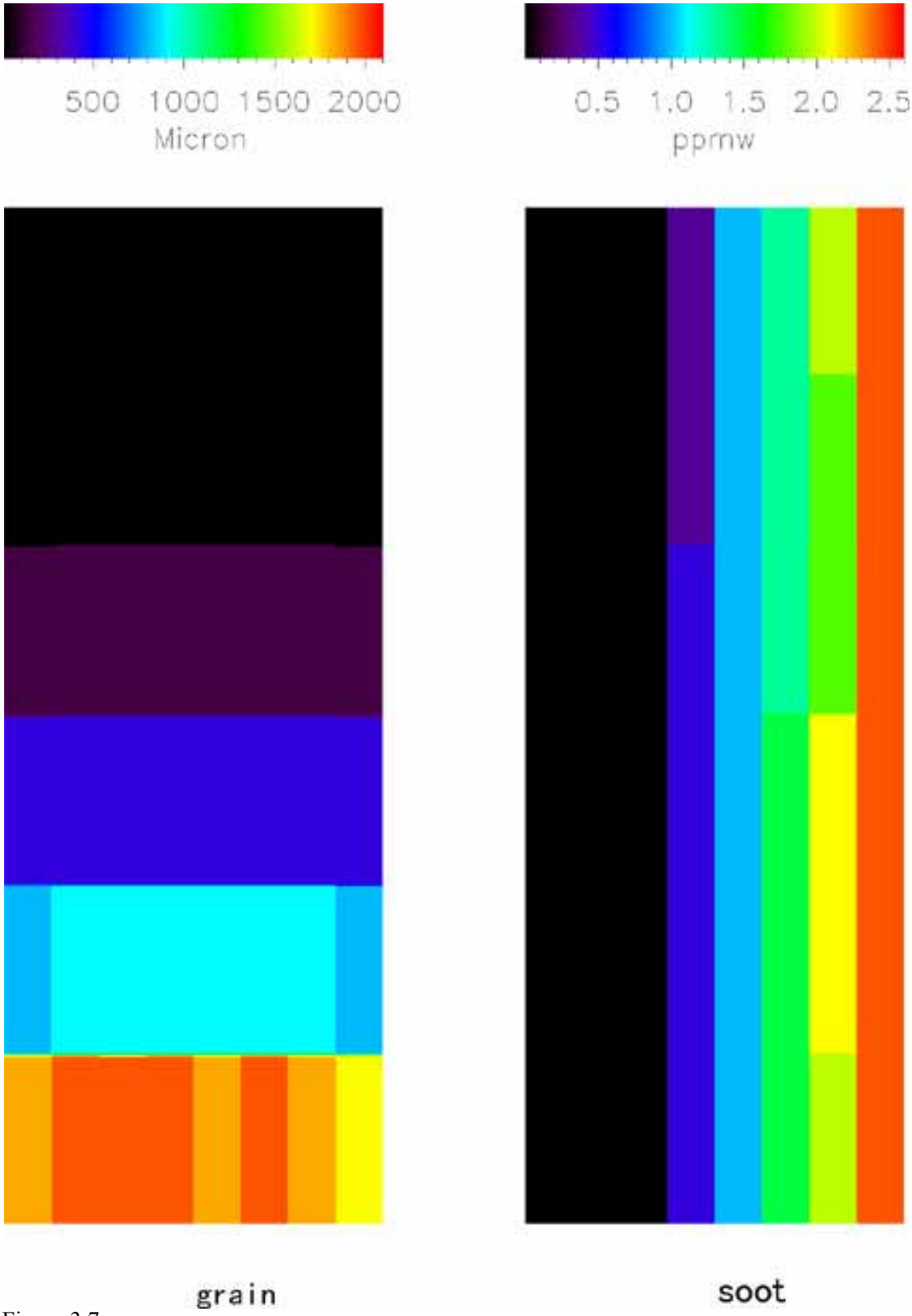

Figure 3.7
Retrieved snow grain size (left panel) and mass fraction of soot mixed in snow (right panel).

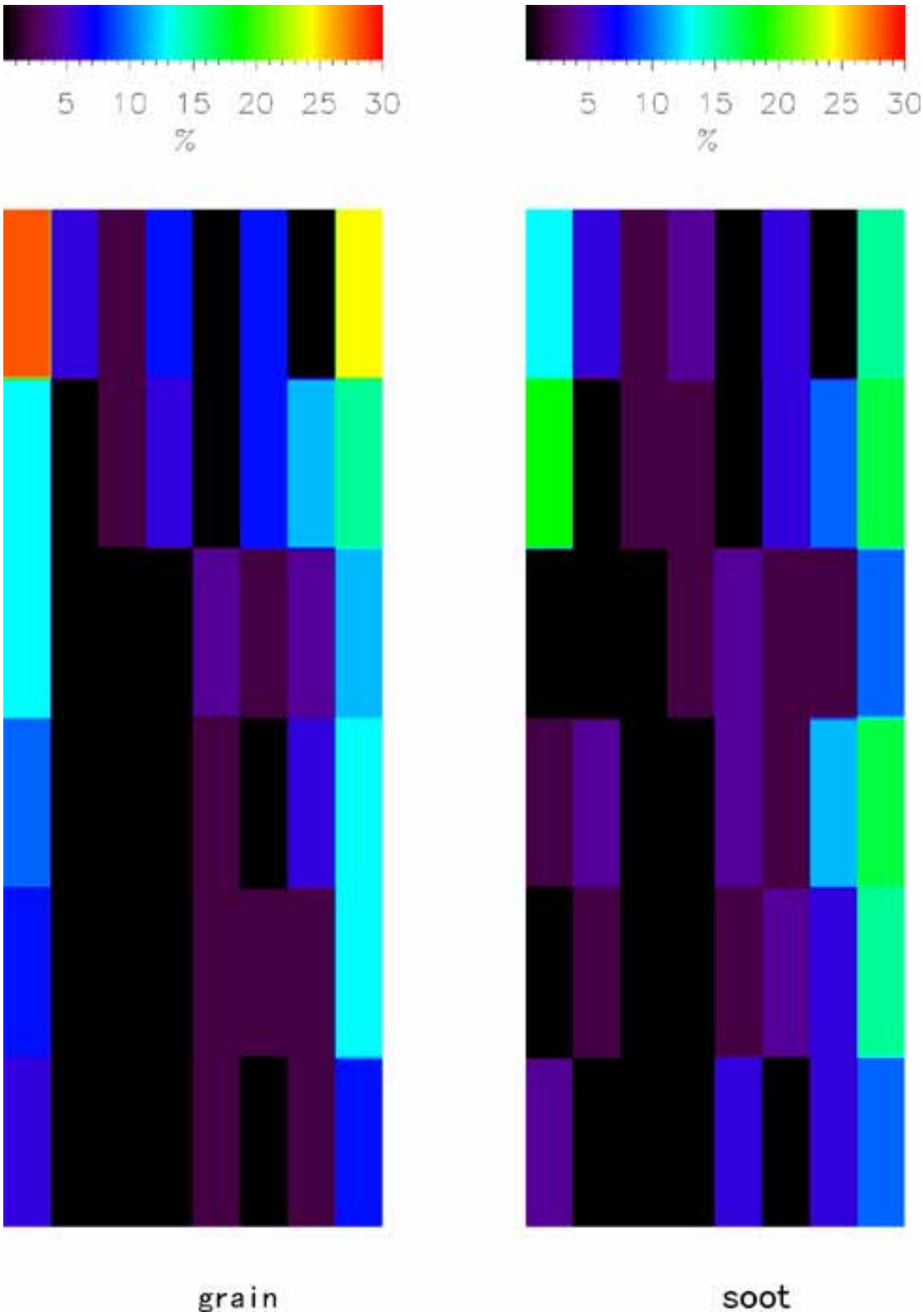

Figure 3.8
The retrieval relative errors for snow grain size (left panel) and mass fraction of soot mixed in snow (right panel).

(3) Quality Control and Diagnostic Information

(4) Exception Handling

(5) Constraints, Limitations, Assumptions

At present time, this algorithm is designed for clear-sky pixels over the polar regions and mid-latitude regions (between 20° and 60° in latitude). For the Arctic and Antarctic regions, the tropospheric aerosol model and Antarctic background aerosol model (Aoki et al., 1999) have been used, respectively. For mid-latitude regions, we adopt five aerosol models from MODTRAN. These aerosol models are: (i) Rural aerosol model with 23 km visibility, (ii) Rural aerosol model with 5 km visibility, (iii) Navy maritime aerosol model with 10 (m/s) wind speed, (iv) Urban aerosol model with 23 km visibility, and (v) Urban aerosol model with 5 km visibility. These aerosol models are not enough to cover all aerosol models existing in mid-latitude area. The accuracy of retrieved snow grain size or soot is mostly determined by the aerosol model selection.

Because we use GLI channel 19 (0.865 μm) to retrieve snow grain size and channel 5 (0.46 μm) to retrieve mass fraction of soot, the retrieved mean grain size and/or soot represent the depth-weighted-averaged values appropriate for the radiation penetration depth of these channels. Model calculations indicate that the penetration depth for these two channels are 3.5-6.5 cm depending on the snow grain size.

(6) Publications and Papers

Li, W., X. Xiong, K. Stamnes, and B. Chen. Snow grain size determination from AVIRIS data over Arctic ocean, Tenth conference on satellite meteorology and oceanography, California, Jan. 9-14, 2000. (extended abstract in press).

D. References

Aoki, Teruo, Tadao Aoki, M. Fukabori, Y. Tachibana, Y. Zaizen, F. Nishio, and T. Oishi, 1998: Spectral albedo observation on the snow field at Barrow, Alaska. *Polar Meterorol. Glaciol.,* **12**, 1–9.

Aoki, Teruo, Tadao Aoki, M. Fukabori, and A. Uchiyama, 1999: Numerical simulation of the atmospheric effects on snow albedo with a multiple scattering radiative transfer model for the atmosphere-snow system. *J. of the Meteor. Soc. of Japan*, **77,** 595–614.

Blanchet, J. and R. List, 1983: Estimation of optical properties of arctic haze using a numerical model. *Atmos. Ocean,* **21,** 444–465.

Bourdelles, B., and M. Fily, 1993: Snow grain-size determination from Landsat imagery over Terre Adelie. Antarctica, *Annals of Glaciology,* **17,** 86–92.

Fily, M., B. Bourdelles, J.P. Dedieu, and C. Sergent, 1997: Comparison of in situ and Landsat Thematic Mapper derived snow grain characteristics in the Alps. *Remote Sens. Environ.,* **59,** 452–460.

Nolin, A.W. and J. Dozier, 1993: Estimating snow grain size using AVIRIS data. *Remote Sens. Environ.,* **44,** 231–238.

Painter, T.H., D.A. Roberts, R.O. Green, and J. Dozier, 1998: The effect of grain size on spectral mixture analysis of snow-covered area from AVIRIS data. *Remote Sens. Environ.,* **65,** 320–332.

Stamnes, K., S.-C. Tsay, W. Wiscombe, and K. Jayaweera, 1988: Numerically stable algorithm for discrete-ordinate-method radiative transfer in multiple scattering and emitting layered media. *Appl. Opt.,* **27,** 2502–2509.

Stamnes, K., 1998: ADEOS-II/GLI Cloudy/clear and snow/sea-ice discriminators for polar regions, Algorithm Theoretical Basis Document (ADEOS-II/GLI), NASDA.

Warren, S.G., 1982: Optical properties of snow. *Rev. Geophys. Space Phys.,* **20,** 67–89.

Warren, S.G. and W.J. Wiscombe, 1980: A model for the spectral albedo of snow. II. Snow containing atmospheric aerosols. *J. Atmos. Sci.,* **37,** 2734–2745.

Wiscombe, W.J. and S.G. Warren, 1980: A model for the spectral albedo of snow. I. Pure snow. *J. Atmos. Sci.,* **37,** 2712–2733.